Wireless Power Transfer, 2018, 5(2), 97–104. © Cambridge University Press, 2018
doi:10.1017/wpt.2018.3

RESEARCH ARTICLE

Effect of tuning capacitance of passive power repeaters on power transfer capability of inductive power transfer systems

RONG HUA AND AIGUO PATRICK HU

Power repeaters are used to extend the power transfer range or enhance the power transfer capability of Inductive Power Transfer (IPT) systems, but how to tune the power repeaters to improve the system power transfer performance remains an unsolved problem. In this paper, studies of the effect of the tuning capacitance of the power repeater of an IPT system on the power transfer capability are presented. A theoretical model is established to analyze the output power of the system with the primary coil and secondary coil tuned at a nominal resonant frequency, and a passive power repeater placed in between. By analyzing the relationship between the tuning capacitance of the power repeater and the output power, a critical tuning capacitance which sets up the boundary between enhancing and reducing the output power is determined, and the optimal tuning capacitances corresponding to the maximum and minimum output power are also obtained. A practical IPT system with a passive power repeater placed at 40, 80, and 104 mm from the primary coil is built. It has shown that the practically measured critical capacitance and the optimal tuning capacitance for maximum power transfer are in good agreement with the analytical results.

Keywords: Inductive power transfer, Passive power repeater

Received 7 February 2018; Revised 14 May 2018; Accepted 11 June 2018; first published online 6 August 2018

I. INTRODUCTION

Wireless power transfer (WPT) is a technology for transferring power when direct wire connection is difficult or impossible. WPT is cataloged into far-field and near-field depending on the system operating frequency and resultant waveform compared to the component size and power transfer distance. Far-field technology uses propagating electromagnetic waves to transfer power, which has been successfully used for RFID [1] and medical implants [2]. However, the system efficiency of a far-field power transfer system is low due to its weak directionality. Inductive power transfer (IPT) is based on near-field coupling, and it has gained successful applications in materials handling [3], biomedical sensors and actuators [4], medical implants [5–8], robots [9, 10], smart grids [11], and building monitoring [12]. In an IPT system, the power transfer capability decreases with the magnetic field coupling because the field strength decays very quickly with the increase of the physical distance between the coupled coils. As a result, the power transfer capability of IPT systems is limited within the frame of a loosely coupled high-frequency transformer.

Large coils [13] and different coil configurations [14] have been used to improve the magnetic field coupling and thereby increasing the power transfer capability. However, practically the coil size is often limited by the physical constraints of a system, and complex coil configurations require complicated control for driving them. Advanced compensation and control techniques have been developed to increase the power transfer capability of loosely coupled IPT systems [15], but the power transfer capability is fundamentally limited by the path of a "magnetic circuit" due to the nature of magnetic field coupling, which cannot be changed by just external circuit compensation and control. Passive power repeaters are proposed to enhance the power transfer capability of IPT systems. They are normally formed by a series LC resonant tank, and placed between a primary transmitter and a power pickup. The power transfer capability of the IPT system is enhanced by strengthening the magnetic field coupling between the primary coil and pick up coil through a relaying magnetic field. Passive power repeaters have been successfully used in applications such as machine tools [16], biomedical implants [17], and building services [18]. The domino effects [19, 20], frequency splitting [21, 22], and power efficiency [23] of IPT systems with passive power repeaters have been studied. However, the passive power repeaters are tuned at the nominal operating frequency, which may not lead to optimal output power performance.

In this paper, study of the effect of the tuning capacitance of a passive power repeater on the power transfer capability of an IPT system is presented. The optimal tuning capacitance corresponding to the system maximum power transfer capability is determined by analytical analysis under the

Department of Electrical and Computer Engineering, The University of Auckland, New Zealand
Corresponding author:
R. Hua
Email: rhua027@aucklanduni.ac.nz

nominal tuning conditions of the primary and secondary coils, together with the tuning boundary between the enhancement and reduction of power transfer. The results can be used to design the tuning capacitance of a power repeater to increase the power transfer capability of an inductive power system, or improve the coupling tolerance of a system at a certain power level. For example, a power repeater can be placed in between a primary coil and secondary coil of a wireless charging system of mobile phones to improve the charging distance and misalignment tolerance. The method can also be used to form a larger charging area for charging multiple devices using a smaller single primary coil.

II. SYSTEM MODELING AND OUTPUT POWER ANALYSIS

Figure 1 shows a layout of an IPT system with a primary transmitter, a passive power repeater, and a power pickup. The power repeater is placed between the primary coil and the power pickup coil for relaying the magnetic field generated by the primary coil to the pickup coil. The primary transmitter contains a DC power supply, a DC–AC inverter, and a primary coil which is series tuned with a capacitor to the nominal frequency. The power repeater is formed by a lumped coil tuned using a capacitor to the frequency of interest. A pickup coil, a load resistor, and a tuning capacitor are in series connected to form the power pickup, and the pickup coil is tuned to the nominal frequency.

The equivalent steady-state circuit model of the IPT system is shown in Fig. 2. The DC power supply and DC–AC inverter is modeled as a constant voltage source. The transmitting coil is modeled as an inductor L_1 with an Equivalent Series Resistance (ESR) R_1, and a capacitor C_1 is added to tune the transmitting coil. The coil of the power repeater is modeled as an inductor L_2 with an ESR R_2, and it is tuned with a capacitor C_2. The power pickup coil is modeled as an inductor L_3 with an ESR of R_3, and it is in series connected with a tuning capacitor C_3 and load resistor R_L. Inductors L_1 and L_2 are magnetically linked by mutual inductance M_{12}. The mutual inductance M_{23} magnetically links inductors L_2 and L_3, and the mutual inductance M_{13} magnetically links inductors L_1 and L_3.

The Kirchhoff's voltage law (KVL) is applied to each resonant circuit of the system:

$$\begin{aligned} &j\omega M_{12}I_2 + j\omega M_{13}I_3 + (X_1 j + R_1)I_1 = V_s \\ &j\omega M_{12}I_1 + j\omega M_{23}I_3 + (X_2 j + R_2)I_2 = 0 \\ &j\omega M_{13}I_1 + j\omega M_{23}I_2 + (X_3 j + R_3 + R_L)I_3 = 0. \end{aligned} \quad (1)$$

where I_1, I_2, and I_3 are the currents going through the primary coil, the coil of power repeater, and the load resistance, respectively, V_s is the input voltage, X_1, X_2, and X_3 are the reactances of the resonant circuit of primary transmitter, the power repeater, and the power pickup, respectively, and they are represented as

$$\begin{aligned} &X_1 = \omega L_1 - \frac{1}{\omega C_1}, \quad X_2 = \omega L_2 - \frac{1}{\omega C_2}, \\ &X_3 = \omega L_3 - \frac{1}{\omega C_3}. \end{aligned} \quad (2)$$

As both the primary coil and the pickup coil are tuned to the nominal frequency, X_1 and X_3 equal to zero. So (2) can be simplified as (3):

$$\begin{aligned} &j\omega M_{12}I_2 + j\omega M_{13}I_3 + R_1 I_1 = V_s \\ &j\omega M_{12}I_1 + j\omega M_{23}I_3 + (X_2 j + R_2)I_2 = 0 \\ &j\omega M_{13}I_1 + j\omega M_{23}I_2 + (R_3 + R_L)I_3 = 0. \end{aligned} \quad (3)$$

By simultaneously solving three equations in (3), the output current is achieved as (4):

$$I_3 = -\frac{M_{12}M_{23}V_s\omega^2 + j\omega M_{13}V_s(R_2 + X_2 j)}{\begin{aligned} &M_{12}^2\omega^2(R_3 + R_L) - 2jM_{12}M_{13}M_{23}\omega^3 + (R_2 + X_2 j)M_{13}^2\omega^2 \\ &+ R_1 M_{23}^2\omega^2 + R_1(R_3 + R_L)(R_2 + X_2 j) \end{aligned}}. \quad (4)$$

By substituting the amplitude of I_3 into (5), the output power is obtained as (6):

$$P_o = |I_3|^2 R_L, \quad (5)$$

$$P_o = \frac{V_s^2\omega^2((M_{13}X_2 - M_{12}M_{23}\omega)^2 + M_{13}^2R_2^2)R_L}{\begin{aligned} &\left(-2M_{12}M_{13}M_{23}\omega^3 + X_2M_{13}^2\omega^2 + R_1X_2(R_3 + R_L)\right)^2 \\ &+ \left(M_{12}^2(R_3 + R_L)\omega^2 + M_{13}^2R_2\omega^2 + M_{23}^2R_1\omega^2 \right. \\ &\left. + R_1R_2(R_3 + R_L)\right)^2 \end{aligned}}. \quad (6)$$

Equation (6) shows the relationship between the output power and the reactance X_2 of the power repeater. For given mutual inductances between the coupled coils, ESRs of coupled coils, load resistance, and a system operating frequency, the

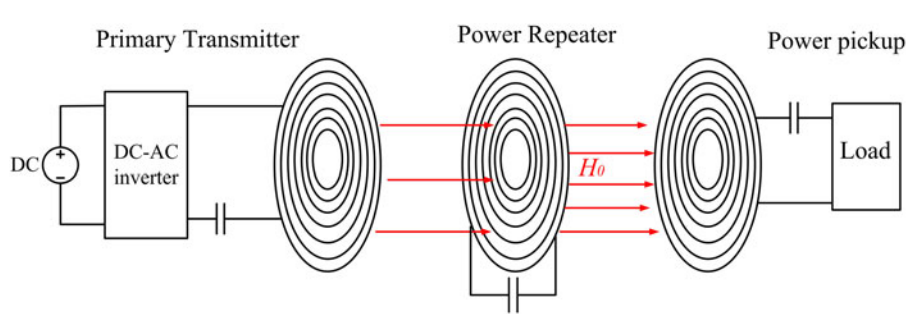

Fig. 1. An overview of a typical layout of an IPT system with a passive power repeater.

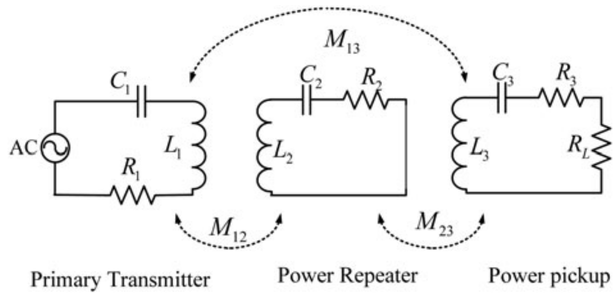

Fig. 2. The equivalent system steady-state circuit model.

relationship between the output power of an IPT system and the reactance of power repeater can be achieved by using optimization tools such as MATLAB.

III. EFFECT OF POWER REPEATER TUNING ON OUTPUT POWER

A) Determining the critical tuning capacitance between enhancing and reducing the output power

The output power of the IPT system without the passive power repeater is set to be the reference for determining whether the output power is enhanced and reduced by the power repeater. For the IPT system without the passive power repeater, the system equation (7) can be derived by applying KVL to the primary and pickup resonant circuits:

$$\begin{aligned} j\omega M_{13} I_{3-noR} + R_1 I_{1-noR} &= V_s \\ j\omega M_{13} I_{1-noR} + R_3 I_{3-noR} &= 0. \end{aligned} \tag{7}$$

where I_{1-noR} and I_{3-noR} are the current going through the primary coil and the load resistance of the IPT system when there is no passive power repeater.

By simultaneously solving two equations in (7), I_{3-noR} is obtained. Multiplying the square of the amplitude of I_{3-noR} by the load resistance R_L, the output power of the IPT system without the power repeater is obtained as

$$P_{o-noR} = \frac{(M_{13}^2 R_L V s^2 \omega^2)}{(\omega^2 M_{13}^2 + R_1 R_3 + R_1 R_L)^2}. \tag{8}$$

The power ratio between P_o and P_{o-noR} is represented as

$$r = \frac{P_o}{P_{o-noR}}. \tag{9}$$

The output power is enhanced by the power repeater when the ratio is larger than 1, and the output power is reduced when the ratio is smaller than 1. By substituting (6) and (8) into (9) and solving (9) when it equals to 1, the critical reactance X_{2-cr} which sets up the boundary between increasing or decreasing of the system output power is obtained as (10). By substituting (10) into (2), the corresponding tuning capacitance is obtained as (11):

$$X_{2-Cr} = \frac{M_{12}^2 M_{23}^2 \omega^2 + M_{13}^2 R_2^2 - \left(M_{13}^2 \left(\begin{array}{l} \left(M_{12}^2 \omega^2 (R_3 + R_L) + M_{13}^2 R_2 \omega^2 + M_{23}^2 R_1 \omega^2 + R_1 R_2 (R_3 + R_L) \right)^2 \\ + 4 M_{12}^2 M_{13}^2 M_{23}^2 \omega^6 \end{array} \right) \Big/ \left(M_{13}^2 \omega^2 + R_1 (R_3 + R_L) \right)^2 \right)}{2 M_{12} M_{13} M_{23} \omega - \left(4 M_{12} M_{13}^3 M_{23} \omega^3 / M_{13}^2 \omega^2 + R_1 (R_3 + R_L) \right)}, \tag{10}$$

$$C_{2-Cr} = \frac{1}{\omega^2 L_2 - \left(\dfrac{M_{12}^2 M_{23}^2 \omega^2 + M_{13}^2 R_2^2 - \left(\begin{array}{l} M_{13}^2 \left(\begin{array}{l} \left(M_{12}^2 \omega^2 (R_3 + R_L) + M_{13}^2 R_2 \omega^2 + M_{23}^2 R_1 \omega^2 + R_1 R_2 (R_3 + R_L) \right)^2 \\ + 4 M_{12}^2 M_{13}^2 M_{23}^2 \omega^6 \end{array} \right) \\ / \left(M_{13}^2 \omega^2 + R_1 (R_3 + R_L) \right)^2 \end{array} \right)}{2 M_{12} M_{13} M_{23} - \left(4 M_{12} M_{13}^3 M_{23} \omega^2 / M_{13}^2 \omega^2 + R_1 (R_3 + R_L) \right)} \right)}, \tag{11}$$

$$\begin{aligned} A = {} & \left(M_{12}^2 R_2 (R_3 + R_L) + M_{23}^2 R_1 R_2 \right) M_{13}^4 \\ & + \left(\frac{M_{12}^4 (R_3 + R_L)^2}{2} + \frac{M_{23}^4 R_1^2}{2} \right) M_{13}^2, \end{aligned}$$

$$\begin{aligned} B = {} & -M_{12}^2 M_{23}^2 R_1^2 (R_3 + R_L)^2 - M_{13}^2 (M_{12}^2 R_1 R_2 (R_3 + R_L)^2 \\ & + M_{23}^2 R_1^2 R_2 (R_3 + R_L)), \end{aligned}$$

$$C = (M_{12}^2 M_{13}^2 \omega^2 + M_{23}^2 R_1^2)(M_{12}^2 (R_3 + R_L)^2 + \omega^2 M_{13}^2 M_{23}^2) \times \begin{pmatrix} (M_{12}^4 M_{13}^2 \omega^4 + 4\omega^2 M_{12}^2 M_{13}^2 R_2 R_1 + \ \omega^2 M_{12}^2 M_{23}^2 R_1^2 \\ + 4M_{13}^2 R_1^2 R_2^2)(R_3 + R_L)^2 + (8\omega^2 M_{13}^4 R_1 R_2^2 + \ 4\omega^2 M_{13}^2 M_{23}^2 R_1^2 R_2 \\ +4\omega^4 M_{12}^2 M_{13}^4 R_2)(R_3 + R_L) + \ M_{13}^2 \omega^4 (2M_{13}^2 R_2 + M_{23}^2 R_1)^2 \\ +M_{12}^2 M_{13}^4 M_{23}^2 \omega^6) \end{pmatrix},$$

$$D = M_{12} M_{13} M_{23}(-M_{13}^4 \omega^4 + R_1^2 (R_3 + \ R_L)^2).$$

Equation (11) shows the critical tuning capacitance which sets up the boundary between increasing and decreasing the output power. By setting (9) to larger than 1 and solving the equation, it is found that the output power is enhanced when the tuning capacitance of a passive power repeater is smaller than the critical capacitance. The output power is found to be reduced when the tuning capacitance of a passive power repeater is larger than the critical tuning capacitance by solving (9) when it is set to be smaller than 1. The finding of the critical tuning capacitance can help to choose the right range of tuning capacitances of passive power repeaters for increasing the output power of the IPT systems.

B) Determining the optimal tuning capacitances

Equations (6) and (8) are substituted into (9), and then the first differentiation of (9) is set as

$$\frac{dr}{dX_2} = 0. \tag{12}$$

By solving (12), the optimal reactances X_{2-op1} and X_{2-op2} of a passive power repeater are obtained as (13):

$$\begin{aligned} X_{2-op1} &= \frac{3\omega M_{12} M_{23}}{2M_{13}} - \frac{(2\omega^3 A - 2\omega B + \sqrt{C})}{2D} \\ X_{2-op2} &= \frac{3\omega M_{12} M_{23}}{2M_{13}} + \frac{(2\omega B - 2\omega^3 A + \sqrt{C}),}{2D} \end{aligned} \tag{13}$$

where the representations of A, B, C, and D are presented above.

To check whether the two optimal capacitances are for achieving the maximum output power, equation (9) is differentiated with respect of X_2 again. By substituting X_{2-op1} and X_{2-op2} into the second differentiation, respectively, it is found that neither of the second differentiations equal to zero, which indicates X_{2-op1} and X_{2-op2} are not inflection points. Therefore, one of them is for achieving maximum output power, and the other one is for obtaining minimum output power.

To determine the optimal tuning capacitance for achieving the maximum output power, the output powers P_{op1} and P_{op2} are obtained by substituting X_{2-op1} and X_{2-op2} into (6), respectively. By subtracting P_{op1} by P_{op2}, (14) is obtained:

$$P_{op1} - P_{op2} = \frac{R_L V_s^2 \omega^3 \sqrt{C}}{\begin{bmatrix} ((\omega^2 M_{13}^2 + R_1(R_3 + R_L))(\omega^2 M_{12}^2 (R_3 + R_L)^2 \\ +\omega^2 M_{13}^2 R_2 + \omega^2 M_{23}^2 R_1 + R_1 R_2 (R_3 + R_L)) \end{bmatrix}^2}. \tag{14}$$

Equation (14) shows the difference between P_{op1} and P_{op2}, and it is found to be positive, which indicates X_{2-op1} is the reactance for achieving maximum output power, and X_{2-op2} is the reactance for obtaining minimum output power. By substituting X_{2-op1} and X_{2-op2} into (2), the corresponding tuning capacitances are obtained as in (15):

$$\begin{aligned} C_{2-P\max} &= \frac{1}{\begin{aligned} &\omega^2 L_2 - ((3\omega^2 M_{12} M_{23}/2M_{13}) \\ &-((2\omega^3 A - 2\omega B + \sqrt{C}) \\ &/2M_{12} M_{13} M_{23}(-M_{13}^4 \omega^4 + R_1^2 (R_3 + \ R_L)^2))) \end{aligned}}, \\ C_{2-P\min} &= \frac{1}{\begin{aligned} &\omega^2 L_2 - ((3\omega^2 M_{12} M_{23}/2M_{13}) \\ &+((2\omega^3 A - 2\omega B + \sqrt{C}) \\ &/2M_{12} M_{13} M_{23}(-M_{13}^4 \omega^4 + R_1^2 (R_3 + \ R_L)^2))) \end{aligned}}. \end{aligned} \tag{15}$$

Equation (15) gives the optimal tuning capacitances corresponding to the maximum and minimum output powers. The maximum output power can be achieved when the tuning capacitance of power repeater equals C_{2-Pmax}, and the minimum output power can be obtained when the tuning capacitance is C_{2-Pmin}.

These two optimal tuning conditions are also related to power enhancing and reducing characteristics of the power repeater. Combining the finding of the range of tuning capacitance for increasing and reducing the output power, Fig. 3 is plotted to illustrate the general relationship between the output power and the tuning capacitance of a passive power repeater, and key tuning capacitances are labeled in the plot. Compared to the original IPT system without a passive power repeater, the output power P_o of the IPT system with a passive power repeater can be higher when the tuning capacitance of power repeater C_2 is smaller than the critical tuning capacitance C_{2-Cr}; and lower when C_2 is larger than C_{2-Cr}. The maximum and minimum output powers are obtained at C_{2-Pmax} and C_{2-Pmin}, respectively. P_o approaches

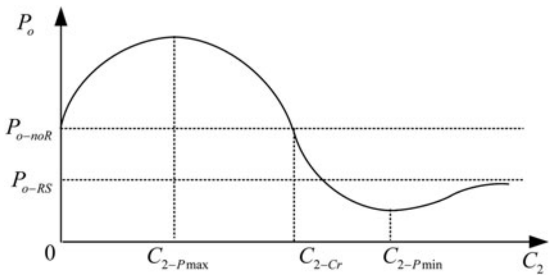

Fig. 3. Illustrations of the general relationship between the output power and the tuning capacitance of the power repeater.

P_{o-RS} as shown in Fig. 3 when the tuning capacitance increases to infinite, corresponding to the situation when the power repeater is short circuited. This research focuses on enhancing the output of the IPT system, so the tuning capacitance of the power repeater is smaller than the critical tuning capacitance C_{2-Cr}.

IV. EXPERIMENTAL VERIFICATION

The experimental setup is shown in Fig. 4. This setup includes a DC power supply, a waveform function generator, an AC linear power amplifier, a frame for holding coupled coils, and a power pickup circuit. The function generator inputs an AC voltage signal with an amplitude of 500 mV and a frequency of 200 kHz into the AC linear power amplifier. The voltage gain of the linear power amplifier was set to be 10 to generate a voltage with an amplitude of 5 V across the terminals of the resonant circuit of the primary transmitter. The resonant frequency of the primary resonant circuit was tuned at 200 kHz. The power repeater was set by connecting a lumped coil with a tuning board which was used to manually change the tuning capacitance. The pickup was built by connecting a lumped pickup coil, a tuning capacitor, and a load resistor in series, and the power pickup was tuned at 200 kHz. The primary coil, the coil of the power repeater, and the pickup coil were made by using telephone cables with 10 turns, with an inner radius of 31.25 mm and an outer radius of 60 mm, and ferrite bars were added at the bottom of the primary and pickup coils. They were placed in the frame which includes two vertical holders with a height of 153 mm and two plates with dimensions of 150 mm × 150 mm. Each vertical holder has 25 even distributed slots on it, and each plate has a tongue on each side. The plates can be put in different vertical positions by being slid into different slots on the holders. The primary coil was placed at the bottom of the frame, and the pickup coil was placed 130 mm away from the primary coil.

Table 1 shows the practical measured circuit parameters. Please note the current limiting resistor is added in the circuit to protect the power amplifier for testing purposes, particularly under fully series tuned conditions which can lead to a very high current. Its resistance is chosen to be very small (making the total ESR of the primary resonant circuit less than 1 Ω) to ensure the normal circuit operation is not much affected. This resistor can be removed in the final system.

In the experiment, the root mean square (RMS) value of input voltage across the resonant circuit of the primary transmitter and the RMS value of the output voltage firstly measured when the power repeater was not added into the system. Then, the power repeater was placed at three different positions which are 40, 80, and 104 mm away from the primary coil, respectively. At each position, the coupling coefficient k_{12} between the primary coil and the coil of power repeater and the coupling coefficient k_{23} between the coil of power repeater and the pickup coil were measured. By substituting the inductances in Table 1 and the measured k_{12}, k_{23}, and k_{13} in (16), the mutual inductances M_{12}, M_{23}, and M_{13} were calculated, respectively for each position. The C_{2-Pmax} and C_{2-Cr} for each position were calculated by substituting M_{12}, M_{23}, and M_{13} and system and circuit parameters in (15) and (11), respectively. Table 2 shows the measured k_{12} and k_{23}, the calculated M_{12} and M_{23}, and the predicted C_{2-Pmax} and C_{2-Cr} of the three positions:

$$M = k\sqrt{L_a L_b}, \tag{16}$$

where M is the mutual inductance between two coupled coils, L_a and L_b are the inductances of two coupled coils, respectively, and k is the coupling coefficient between two coupled coils.

Table 2 shows that C_{2-Pmax} is smaller than C_{2-cr} for all three positions. Therefore, the tuning capacitance of the power repeater was manually varied from a tuning capacitance smaller than C_{2-Pmax} to a tuning capacitance larger than C_{2-Cr} at each position. Both the RMS values of the output voltage and the input voltages across the resonant

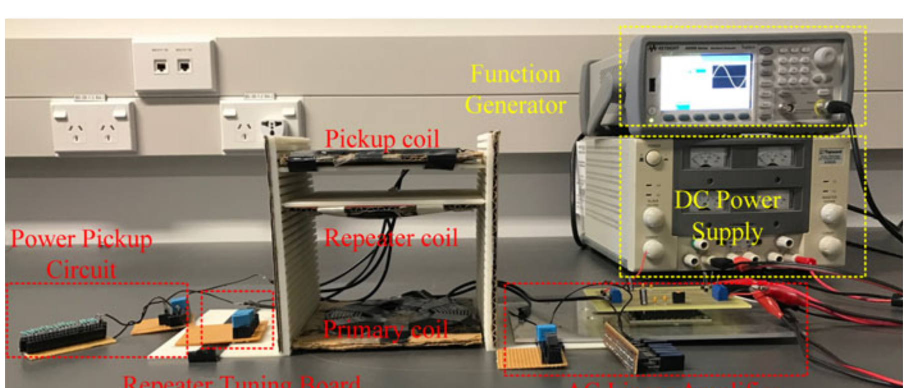

Fig. 4. The experimental setup.

Table 1. The practical system and circuit parameters.

Parameters	Value
f_0	200 kHz
V_s (RMS)	3.55 V
L_1	17.427 μH
L_2	12.15 μH
L_3	17.79 μH
R_1 (including the current limiting resistor)	0.66 Ω
R_2	0.263 Ω
R_3	0.208 Ω
R_L	4.8 Ω
C_1	36.3 nF
C_3	35.6 nF

circuit of the primary transmitter were measured for all tuning capacitances within the range of the variation.

Due to the reflected effects from the passive power repeater and the power pickup, the RMS value of the input voltage from the AC power linear amplifier slightly changed when the tuning capacitance was manually varied. The input voltage was calibrated by dividing 3.55 V which is the input voltage when the power repeater was not added into the system for each measurement. The measured output voltage was calibrated by dividing the ratio between the input voltage and 3.55 V, and the output power was calculated by using the calibrated output voltage. The ratios between the output power of the IPT system with and without the passive power repeater were obtained. Figures 5–7 show measured and predicted output power ratios in relation to the tuning capacitance of the passive power repeater when the passive power repeater was placed at 40, 80, and 104 mm away from the primary coil, respectively.

Figure 5 shows that the measured output power ratios are in good agreement with the predicted power ratios when the passive power repeater was placed 40 mm away from the primacy coil. The maximum measured power ratio of 1.05 was achieved when the tuning capacitance of power repeater is between 2.3 and 2.5 nF, and the predicted tuning capacitance is 2.43 nF which is 5.65% larger than 2.3 nF. The measured critical tuning capacitance for enhancing and reducing the output power is 4.3 nF which is 10% smaller than its predicted value of 4.73 nF.

Figure 6 shows that the measured power ratios are consistent with the predicted power ratios when the passive power repeater was placed 80 mm away from the primary coil. The output power was maximized by around 71.9% at 37.6 nF which is 2.73% larger than the predicted tuning capacitance of 36.6 nF. The measured critical tuning capacitance is 54 nF which is 0.55% smaller than its predicted value of 54.3 nF.

Figure 7 shows that the measured power ratios are in good agreement with the predicted power ratios when the passive

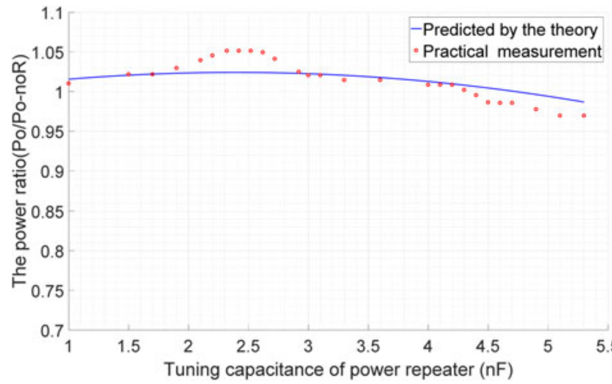

Fig. 5. The measured and predicted output power ratios at tuning capacitances within the range between 1 and 5.3 nF when the passive power repeaters is placed 40 mm away from the primary coil.

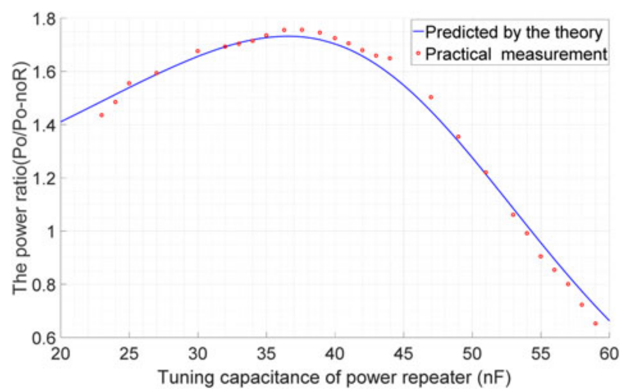

Fig. 6. The measured and predicted output power ratios at tuning capacitances within the range between 20 and 60 nF when the passive power repeater is placed 80 mm away from the primary coil.

power repeater was placed 104 mm away from the primary coil. The output power was maximized by 122% when the tuning capacitance equals to 41 nF which is 1% off from the predicted capacitance of 41.4 nF, and output power ratio is approximately equal to one when the tuning capacitance is 61 nF which is 0.66% smaller than the predicted tuning capacitance of 61.4 nF.

Figures 5–7 show the maximum power transfer ratio changes with the position of the power repeater. The position of a power repeater with a fixed tuning condition has been determined for maximum power transfer efficiency in [24, 25], and the analytical result in relation to the position was obtained by ignoring the mutual inductance between the primary coil and pickup coil. The relationship between the system output power and the position of the power repeater becomes more complicated in the system presented in this paper after considering the mutual inductance between the

Table 2. The measured coupling coefficients, calculated mutual inductances, predicted critical tuning capacitances, and optimal tuning capacitances for obtaining the maximum output power.

The distance between the primary coil and the power repeater (mm)	k_{12}	k_{23}	k_{13}	M_{12} (μH)	M_{23} (μH)	M_{13} (μH)	C_{2-Pmax} (nF)	C_{2-Cr} (nF)
40	0.33	0.057	0.029	4.802	0.838	0.5106	2.4	4.73
80	0.113	0.13	0.029	1.644	1.911	0.5106	36.6	54.3
104	0.0612	0.267	0.029	0.891	3.925	0.5106	41.4	61.4

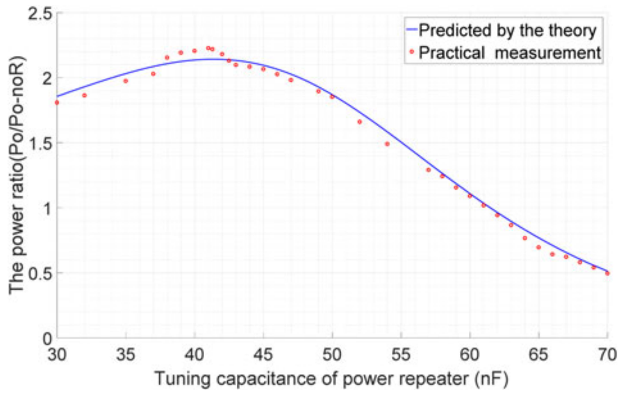

Fig. 7. The measured and predicted output power ratios at tuning capacitances within the range between 30 and 70 nF when the passive power repeater is placed 104 mm away from the primary coil.

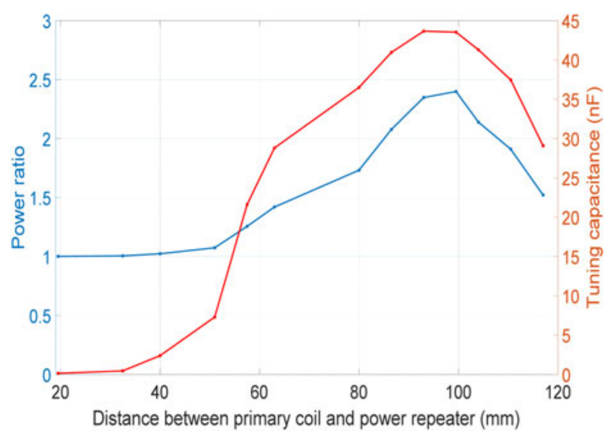

Fig. 8. The relationship between the power ratio and distance between the primary coil and power repeater.

primary coil and pickup coil. Furthermore, to obtain the maximum power transfer, the tuning capacitance of the power repeater needs to be varied away from the nominal tuning capacitance at different positions of the power repeater. To obtain the relationship between the output power and the position of the power repeater, the mutual inductances M_{12} and M_{13} at 13 positions between the primary coil and the power repeater are practically measured, then the maximum output power ratios (with respect to the output power without using a power repeater) are calculated for each position, as shown in Fig. 8, together with the tuning capacitance variations.

It can be seen from Fig. 8 that the maximum output power increases with the increase of the distance between the primary coil and the power repeater until it reaches about 100 mm, and then the output power decreases when the repeater approaches the power pickup. The power ratio reaches the maximum value of about 2.4 when the tuning capacitance of the power repeater is close to 43 nF.

V. CONCLUSION

In this paper, the study of the relationship between the output power of an IPT system and the tuning capacitance of a passive power repeater placed between a primary and a secondary coil tuned at a nominal frequency has been presented. By system modeling and analysis, the critical tuning capacitance of the power repeater corresponding to the boundary between enhancing and reducing the power transfer capability has been determined, and the optimal tuning capacitance for achieving the maximum output power has been found. The power ratios between the output power with and without the power repeater have been practically measured when the power repeater is placed at 40, 80, and 104 mm from the primary coil. Experimental results have shown a good agreement with the theoretical analysis. The measured critical tuning capacitances and the optimal tuning capacitances are close to the predicted values, with the maximum errors of 10 and 5.65%, respectively. The output power was increased by around 71.9% when the power repeater was placed at the middle point between the primary coil and pickup coil. The findings from this research regarding the critical and optimal tuning capacitance can be used to guide the practical tuning design of a passive power repeater of an IPT system.

REFERENCES

[1] Sample, A.P.; Yeager, D.J.; Powledge, P.S.; Mamishev, A.V.; Smith, J.R.: Design of an RFID-based battery-free programmable sensing platform. IEEE Trans. Instrum. Meas., **57** (2008), 2608–2615.

[2] Das, R.; Yoo, H.: A multiband antenna associating wireless monitoring and Nonleaky wireless power transfer system for biomedical implants. IEEE Trans. Microwave Theory Tech., **65** (2017), 2485–2495.

[3] Chen, L.J.; Boys, J.T.; Covic, G.A.: Power management for multiple-pickup IPT systems in materials handling applications. IEEE J. Emerging Sel. Topics Power Electron., **3** (2015), 163–176.

[4] Si, P.; Hu, A.P.; Malpas, S.; Budgett, D.: A frequency control method for regulating wireless power to implantable devices. IEEE Trans. Biomed. Circuits Syst., **2** (2008), 22–29.

[5] Lee, G.; Gwak, H.; Kim, Y.-S.; Park, W.-S.: Wireless power transfer system for diagnostic sensor on rotating spindle, in *2013 IEEE Wireless Power Transfer (WPT)*, 2013, 100–102.

[6] Si, P.; Hu, A.P.; Budgett, D.; Malpas, S.; Yang, J.; Gao, J.: Stabilizing the operating frequency of a resonant converter for wireless power transfer to implantable biomedical sensors, in *Proc. 1st Int. Conf. Sensing Technology*, 2005, 477–482.

[7] McCormick, D.; Hu, A.P.; Nielsen, P.; Malpas, S.; Budgett, D.: Powering implantable telemetry devices from localized magnetic fields, in *2007 29th Annual International Conference of the IEEE Engineering in Medicine and Biology Society*, 2007, 2331–2335.

[8] Dissanayake, T.D.; Hu, A.P.; Malpas, S.; Bennet, L.; Taberner, A.; Booth, L. et al.: Experimental study of a TET system for implantable biomedical devices. IEEE Trans. Biomed. Circuits Syst. **3** (2009), 370–378.

[9] Yan, G.; Ye, D.; Zan, P.; Wang, K.; Ma, G.: Micro-robot for endoscope based on wireless power transfer, in *International Conference on Mechatronics and Automation, 2007. ICMA 2007*, 2007, 3577–3581.

[10] Hu, A.P.; Liu, C.; Li, H.L.: A Novel Contactless Battery Charging System for Soccer Playing Robot, in *2008 15th International Conference on Mechatronics and Machine Vision in Practice*, 2008, 646–650.

[11] Kukde, A.; Mattigiri, S.; Singh, V.; Warty, C.; Wagh, S.: Resonance-based Wireless Power Transfer for smart grid systems, in *2014 IEEE Aerospace Conference*, 2014, 1–6.

[12] Salas, M.; Focke, O.; Herrmann, A.S.; Lang, W.: Wireless power transmission for structural health monitoring of fiber-reinforced-composite materials. IEEE Sensors J., **14** (2014), 2171–2176.

[13] Kurs, A.; Karalis, A.; Moffatt, R.; Joannopoulos, J.D.; Fisher, P.; Soljačić, M.: Wireless power transfer via strongly coupled magnetic resonances. Science, **317** (2007), 83–86.

[14] Zaheer, A.; Hao, H.; Covic, G.A.; Kacprzak, D.: Investigation of multiple decoupled coil primary pad topologies in lumped IPT systems for interoperable electric vehicle charging. IEEE Trans. Power Electron., **30** (2015), 1937–1955.

[15] Wang, B.; Hu, A.P.; Budgett, D.: Power flow control based solely on slow feedback loop for heart pump applications. IEEE Trans. Biomed. Circuits Syst., **6** (2012), 279–286.

[16] Hua, R.; Hu, A.P.; Su, Y.: Three-stages magnetic field repeater for extending the range of inductive power transfer. Trans. China Electrotech. Soc., (2015), 133–137.

[17] Yi, Y.; Buttner, U.; Fan, Y.; Foulds, I.G.: Design and optimization of a 3-coil resonance-based wireless power transfer system for biomedical implants. Int. J. Circuit Theory Appl., **43** (2014), 1379–1390.

[18] Nguyen, M.Q.; Dubey, S.; Rao, S.; Chiao, C.: Wireless power transfer via air and building materials using multiple repeaters, in *2014 Texas Symposium on Wireless and Microwave Circuits and Systems (WMCS)*, 2014, 1–4.

[19] Zhong, W.; Lee, C.K.; Hui, S.: Wireless power domino-resonator systems with noncoaxial axes and circular structures. IEEE Trans. Power Electron., **27** (2012), 4750–4762.

[20] Hao, J.; Wang, J.; Liu, X.; Padilla, W.J.; Zhou, L.; Qiu, M.: High performance optical absorber based on a plasmonic metamaterial. Appl. Phys. Lett., **96** (2010), 251104.

[21] Sample, A.P.; Meyer, D.T.; Smith, J.R.: Analysis, experimental results, and range adaptation of magnetically coupled resonators for wireless power transfer. IEEE Trans. Ind. Electron., **58** (2011), 544–554.

[22] Ahn, D.; Hong, S.: A study on magnetic field repeater in wireless power transfer. IEEE Trans. Ind. Electron., **60** (2013), 360–371.

[23] Zhong, W.X.; Zhang, C.; Liu, X.; Hui, S.Y.R.: A methodology for making a three-coil wireless power transfer system more energy efficient than a Two-coil counterpart for extended transfer distance. IEEE Trans. Power Electron., **30** (2015), 933–942.

[24] Kiani, M.; Jow, U.-M.; Ghovanloo, M.: Design and optimization of a 3-coil inductive link for efficient wireless power transmission. IEEE Trans. Biomed. Circuits Syst., **5** (2011), 579–591.

[25] Niu, W.; Wang, J.; Chu, J.; Gu, W.: Optimal single relay position of a 3-coil wireless power transfer system. –J. Eng., **2016** (2016), 249–252.

Rong Hua graduated from the University of Auckland, New Zealand, with B.E. (Honours) degree in Electrical and Electronic Engineering in 2013. Currently he is pursuing his Ph.D. degree at the Department of Electrical and Computer Engineering, the University of Auckland. His research interests include wireless power transfer, inductive power transfer, and magnetic field power repeaters.

Aiguo Patrick Hu graduated from Xian Jiaotong University, China, with B.E. and M.E. degrees in Electrical Engineering in 1985 and 1988, respectively. He received his Ph.D. from the University of Auckland in 2001 in Electrical and Electronic Engineering, and visited National University of Singapore (NUS) for a semester as an exchange postdoc research fellow. He has published 260 peer-reviewed journal and conference papers with about 4500 citations, authored the first monograph on inductive power transfer technology, and contributed four book chapters on wireless power transfer modeling and control, as well as electrical machines. He has been awarded the University of Auckland VC's Funded Research and Commercialization Medal in April 2017. Patrick is now a full professor in the Department of Electrical and Electronic Engineering, the University of Auckland, and his research interests include wireless/contactless power transfer systems, and application of power electronics in renewable energy systems.